

BIO-OPTICS FOR OCEAN COLOR REMOTE SENSING
OF THE BLACK SEA
(Black Sea Color)

TN12: Satellite ocean color data validation

<i>Workpackage:</i>	4	<i>Satellite products validation and algorithm development</i>
<i>Author(s):</i>	<i>V. Slabakova</i>	<i>IO-BAS</i>

Programme for European Cooperating States (PECS)
ESA contract №4000123951/18/NL/SC
TN12 Satellite ocean color data validation

Document Log

<i>Date</i>	<i>Author</i>	<i>Changes</i>	<i>Version</i>	<i>Status</i>
<i>09.05.2020</i>	<i>Slabakova</i>		<i>V1.0</i>	<i>Draft</i>
<i>13.05.2020</i>		<i>Revisions provided by Dr. G. Zibordi</i>	<i>V 1.1</i>	<i>Draft</i>
<i>14.05.2020</i>	<i>Slabakova</i>		<i>V1.2</i>	<i>Final</i>

1. Introduction

Calibration and validation of the various ocean color products in open-sea and coastal waters are critical element of satellite ocean color missions [Hooker et al., 2000]. The most fundamental of the quantities determined from space are the water-leaving radiance L_w and the remote sensing reflectance R_{rs} (i.e., the ratio of water-leaving radiance to downward irradiance). The uncertainties of these primary ocean color products may affect the subsequent estimation of optical (e.g., absorption and back-scattering coefficients) and biogeochemical products (e.g., chlorophyll (Chl) and Total Suspended Matter (TSM) concentrations), which further may challenge the results of marine environmental and climate studies.

The objective of this report is to evaluate the Ocean and Land Colour Instrument (OLCI) Level-2 ocean color data products for the Black Sea characterized by high bio-optical complexity (from oligo- mesotrophic open sea to eutrophic coastal waters and hypereutrophic Danube delta region). The analyses are focused on full resolution (FR), Non-Time- Critical (NTC) data from Ocean and Land Colour Instrument operated on-board Sentinel-3A. The accuracy of OLCI radiometric and geophysical products were assessed on the base of *in situ* data obtained from: 1) Galata AERONET–OC site [Zibordi et al., 2009] and 2) Black Sea Bio-Opt 2019 [Deliverable TN3, 2019] and national monitoring programme campaigns.

2. Data and Method

2.1 Satellite data

For the matchup analysis Level-2 data full-resolution (FR 300 m/pixel), mode “Non Time Critical” Processing Baseline 2.23 [EUMETSAT, 2018a, 2018b] for the period 26 April 2016 – 29 November 2017 over the western Black Sea were obtained from Copernicus Online Data Access Reprocessed archive (CODAREP - <https://codarep.eumetsat.int/>). The operational OLCI Level 2 FR mode “Non Time Critical” data from 30 November 2017 to August 2019 for the same geographic domain were downloaded from the EUMETSAT Data Centre (<https://archive.eumetsat.int/usc/>).

The OLCI spectral reflectance data ρ_w were converted to normalized water-leaving radiance L_{wn} according to:

$$L_{wn} = \rho_w E_0 / \pi$$

where E_0 is mean extraterrestrial solar irradiance [Thuiller et al., 2003].

2.2 *In situ* data

- **Galata AERONET-OC radiometric data**

The normalized water-leaving radiances (L_{wn}) from the Galata AERONET–OC site for the period April 2016 - August 2019 were applied to validate OLCI L2 primary ocean color radiometric products. The data were obtained from AERONET Ocean Color web site (https://aeronet.gsfc.nasa.gov/new_web/ocean_color.html). The matchup analyses were based on fully quality controlled AERONET-OC Level 2.0 radiometric products [Zibordi et al., 2009].

- **Ship observation**

Quality controlled *in situ* data - $L_{wn}(\lambda)$, Chlorophyll a (Chla), TSM and Colored dissolved organic matter (CDOM) absorption- a_{ys} and absorption by non-pigmented particulate matter – a_{nnp} collected during Black Sea Bio-Opt 2019 campaign were used for validation of OLCI L2 FR standard products. Additionally, in order to increase the number of matchups, data collected during national monitoring campaigns and EUROFLEET BIO-OPT cruise in 2016 were included in the analyses.

2.3 Match-Up Construction

The match-up constructions were obtained from arithmetic average of valid OLCI full-resolution data calculated over the box of 3×3 – image elements centered on the measurements location. These OLCI averages were discarded when data: 1) were affected by the main OLCI standard flags: CLOUD, CLOUD_AMBIGUOUS, CLOUD_MARGIN, INVALID, COSMETIC, SATURATED, SUSPECT, HISOLZEN, HIGHGLINT, SNOW_ICE, AC_FAIL, WHITECAPS, ANNOT_ABSO_D, ANNOT_MIXR1, ANNOT_TAU06, RWNEG_O2, RWNEG_O3, RWNEG_O4, RWNEG_O5, RWNEG_O6, RWNEG_O7, RWNEG_O8 [EUMETSAT, 2018a] with exception of ANNOT flags [Zibordi et al., 2018]; 2) sensor and sun zenith angles were greater than 60° and $< 70^\circ$, respectively; 3) the time window between *in situ* measurements and satellite overpass were higher than ± 3 h; 4) the coefficients of variation of all 9 pixels within the box were higher than 0.2. Finally, the percentage of valid pixels in each box was checked, and when this percentage was no less than 50%, the mean values of the valid pixels in the box was calculated and compared to the *in situ* data. The matchup construction workflow is presented on Figure 1.

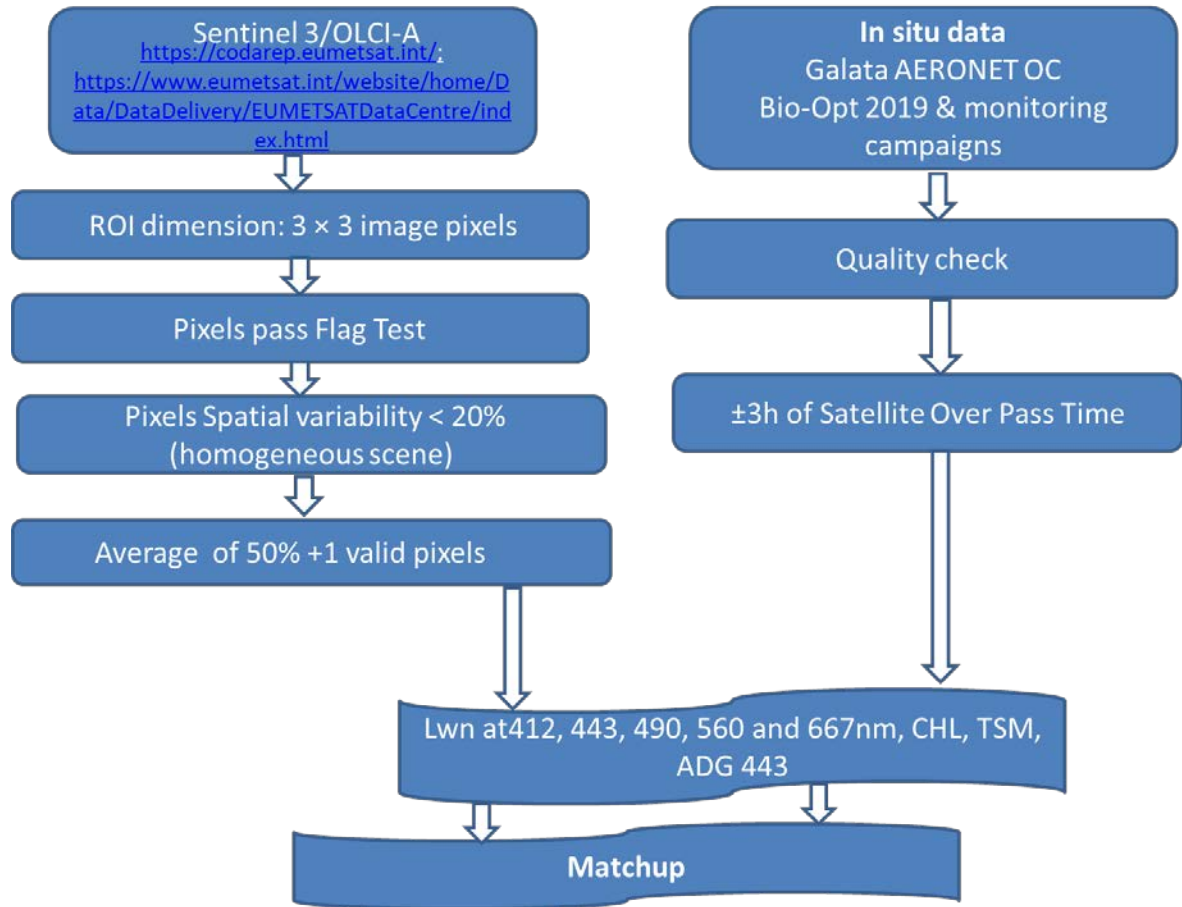


Figure 1. Matchup Construction

2.4 Statistical Method

OLCI L2 ocean color products were evaluated by means of standard statistical quantities including coefficient of determination R^2 , root-mean-square error (RMSE), Mean Percentage Difference (MPD), Mean Absolute Percentage Difference (MAPD).

The values of RMSE, MPD and MAPD are calculated through:

$$RMSE = \sqrt{\frac{\sum_{i=1}^n (X_i - Y_i)^2}{n}}$$

$$MPD = \left(\frac{1}{n} \sum_{i=1}^n \frac{X_i - Y_i}{Y_i} \times 100 \right)$$

$$MAPD = \left(\frac{1}{n} \sum_{i=1}^n \left| \frac{X_i - Y_i}{Y_i} \right| \times 100 \right)$$

where X_i corresponds to satellite data and Y_i indicates the *in situ* data, while n is the number of matchup data points. The RMSE quantifies the error of OLCI data, MPD estimates the deviation and MAPD dispersion between two data sets, and coefficient of determination R^2 indicates the determination coefficient of the linear regression between satellite and *in situ* data. The log_RMSE is used for the assessment of S3/OLCI CHL_OC4ME, CHL_NN, TSM and ADG443 products.

3. Results

3.1 Assessment of the OLCI/Sentinel 3A primary ocean color products

The accuracy of OLCI radiometric products was assessed on the *in situ* data obtained from: 1) Galata AERONET–OC site and 2) ship observations. The analyses were done separately for each data set.

- **Galata $L_{wn}(\lambda)$ vs OLCI $L_{wn}(\lambda)$ data**

The matchup analysis of Galata and satellite L_{wn} spectra were restricted to the bands for which *in situ* data exist (i.e., those identified by the center wavelengths at 412, 443, 490, 560, and 665 nm).

The comparison between the two data sets benefited of 115 matchups. The results related to the assessment of OLCI primary ocean color radiometric products are summarized in Table 1, while the spectral plots and scatter plots for each spectral band of OLCI FR data versus *in situ* AERONET-OC data are presented on Figures 2 and 3.

The comparison of matchup spectra and their averages and standard deviations indicates qualitative agreement between the satellite and AERONET-OC water-leaving radiances, with exception of OLCI L_{wn} data in the blue spectral bands, especially at 412 and 443 nm, where negative values frequently occur (Fig. 2).

The spectra of Galata and OLCI radiance data show exceptionally high L_{wm} values for both *in situ* and satellite data in June 2017. The phytoplankton data collected on 23.05.2017 during an IO-BAS monitoring cruise in the area around Galata platform confirmed the presence of coccolithophore *Emiliana huxleyi* with abundance of $2\ 265\ 120\ \text{cells l}^{-1}$ during the initial phase of the bloom.

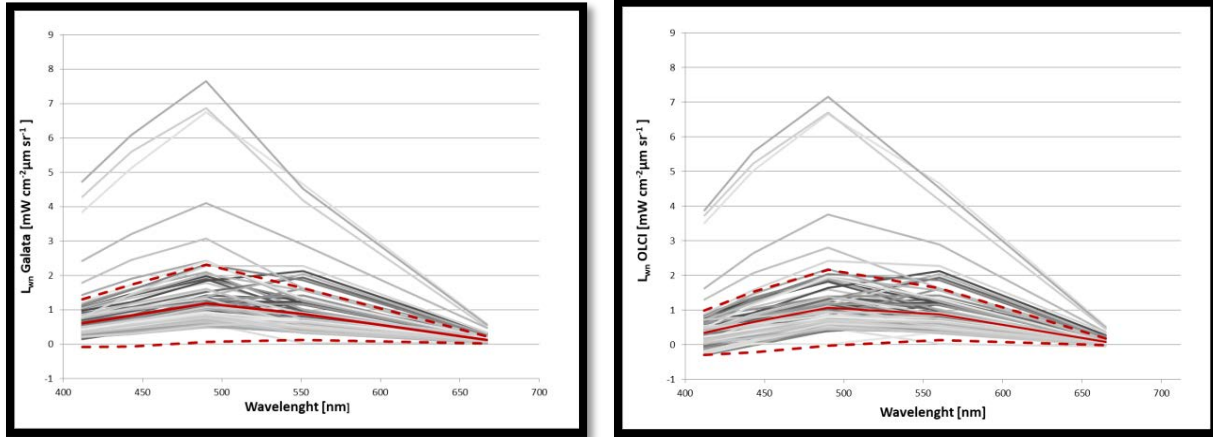


Figure 2. (Left) *in situ* L_{wm} and (Right) OLCI L_{wn} spectra for the Galata matchups. The red continuous lines indicate the spectral averages and the red dashed lines indicate \pm one standard deviation.

Generally, there is a good correlation between OLCI L_{wn} and Galata records for all the wavelengths (Fig. 3). The coefficient of determination R^2 varies from 0.84 at 665 nm to 0.98 at 490 and 560 nm, indicating that most of the OLCI data products appear to agree with the *in situ* data. Still, a significant number of OLCI negative L_{nw} values are observed at 412, 443 nm and 665 nm. This indicates that OLCI L_{wn} data are likely underestimated. The highest RMSE of 0.37 $mW\ cm^{-2}\ \mu m^{-1}\ sr^{-1}$ is determined for L_{wn} at 412 nm that considerably decrease to 0.07 for L_{wn} at 665 nm, in agreement with the lower L_{wn} values. The lower MPD values of -10.63% and -11.20% are estimated at 490 and 560 nm, respectively.

Table 1. OLCIL $L_{wn}(\lambda)$ data statistics

λ	MPD	MAPD	RMSE	R^2
412	-47.11	72.7	0.37	0.85
443	-24.06	39.22	0.27	0.95
490	-10.63	17.21	0.19	0.98
560	-11.20	14.80	0.29	0.98
665	-42.89	52.10	0.07	0.84

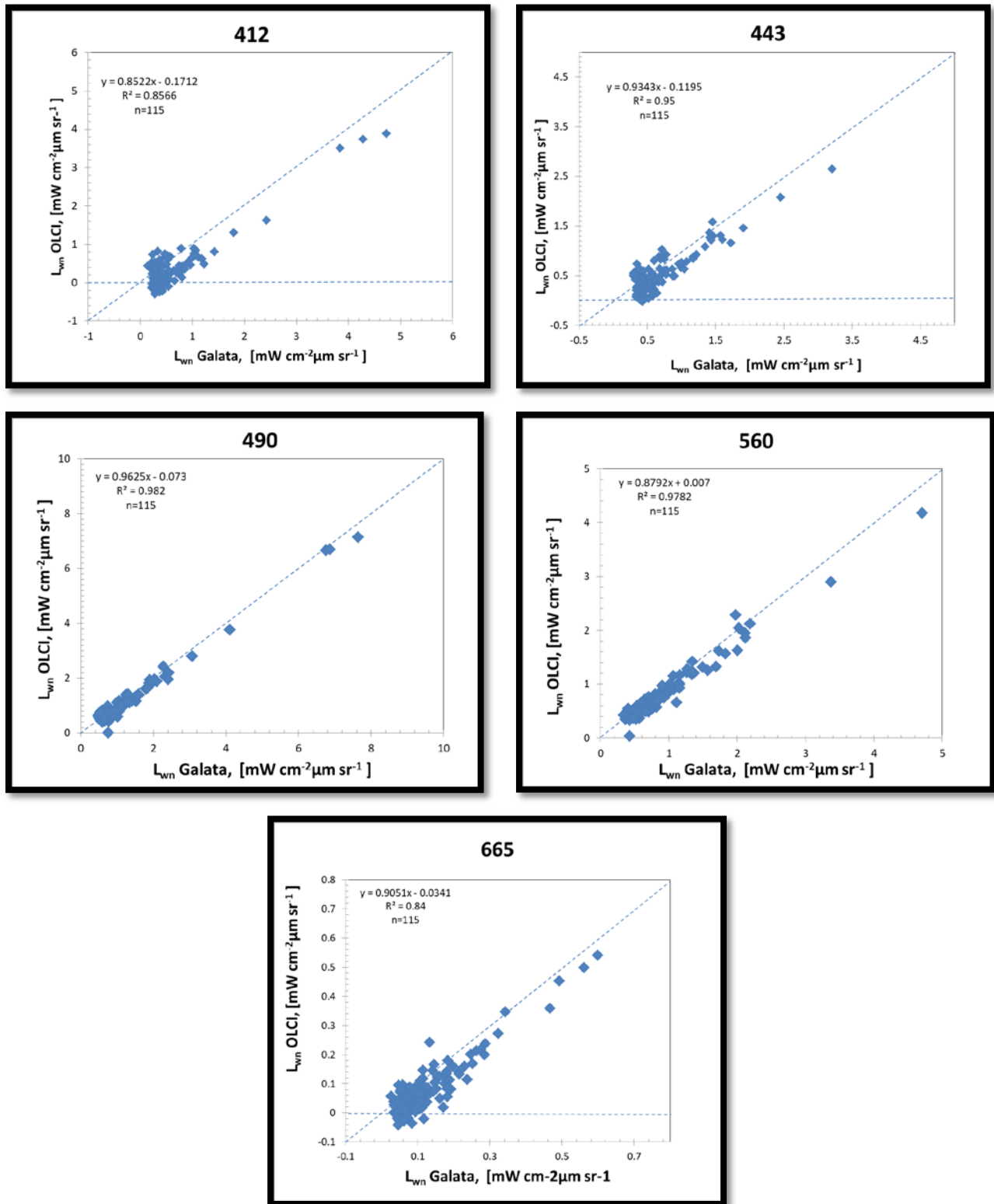


Figure 3. Scatter plots of OLCI and Galata AERONET OC L_{wn} matchup data at 412, 443, 490, 560, and 665 nm

In general, the OLCI normalized water-leaving radiances appear underestimated with respect to the *in situ* data from Galata AERONET-OC site: this is more significant at 412, 443 and 665 nm.

- ***In-water radiometric $L_{wn}(\lambda)$ observations vs OLCI L2 $L_{wn}(\lambda)$ data***

The comparison of *in situ* and satellite L_{wn} spectra restricted to the bands for which *in situ* data exist (i.e., those identified by the center wavelengths at 412, 443, 490, 510, 560, and 665 nm). The total number of matchups is 13 (Tab. 4). The results related to the assessment of OLCI primary ocean color radiometric products in respect to the in-water radiometric observations are summarized in Table 3, while the spectral plots and scatter plots for each spectral band of OLCI L2 FR data versus ship measurements are presented on Figures 3 and 4.

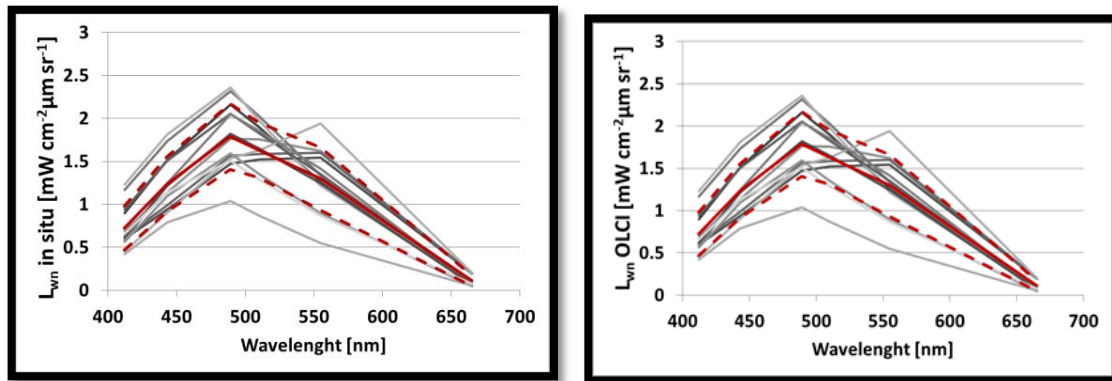
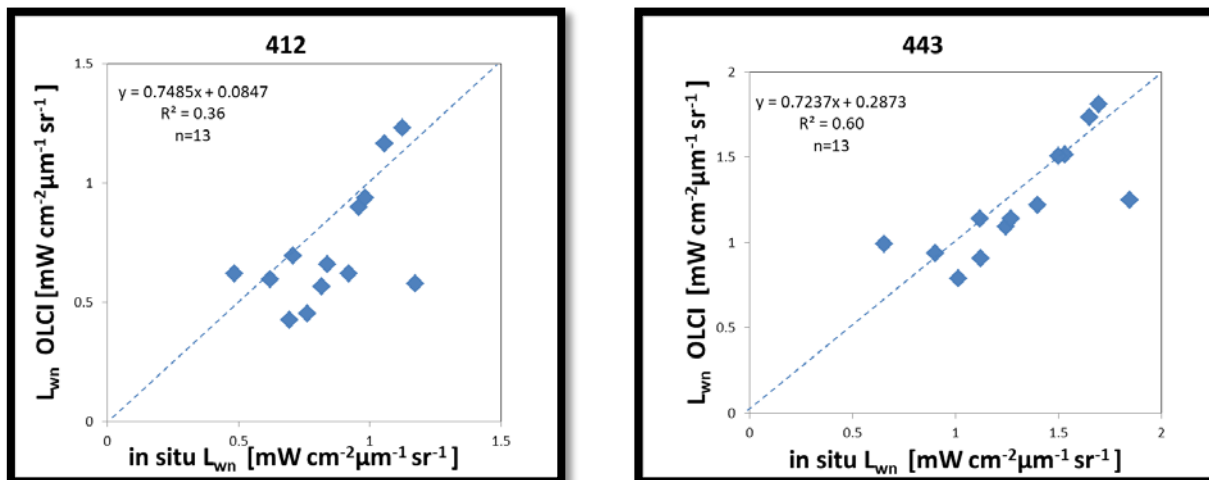


Figure 3. (Left) *in situ* L_{wn} and (Right) OLCI L_{wn} spectra for the sea-truth data matchups. The red continuous lines indicate the spectral averages and the red dashed lines indicate \pm one standard deviation.

The comparison of matchup spectra and their averages and standard deviations indicates qualitative agreement between the satellite and *in situ* water-leaving radiances (Fig. 3).



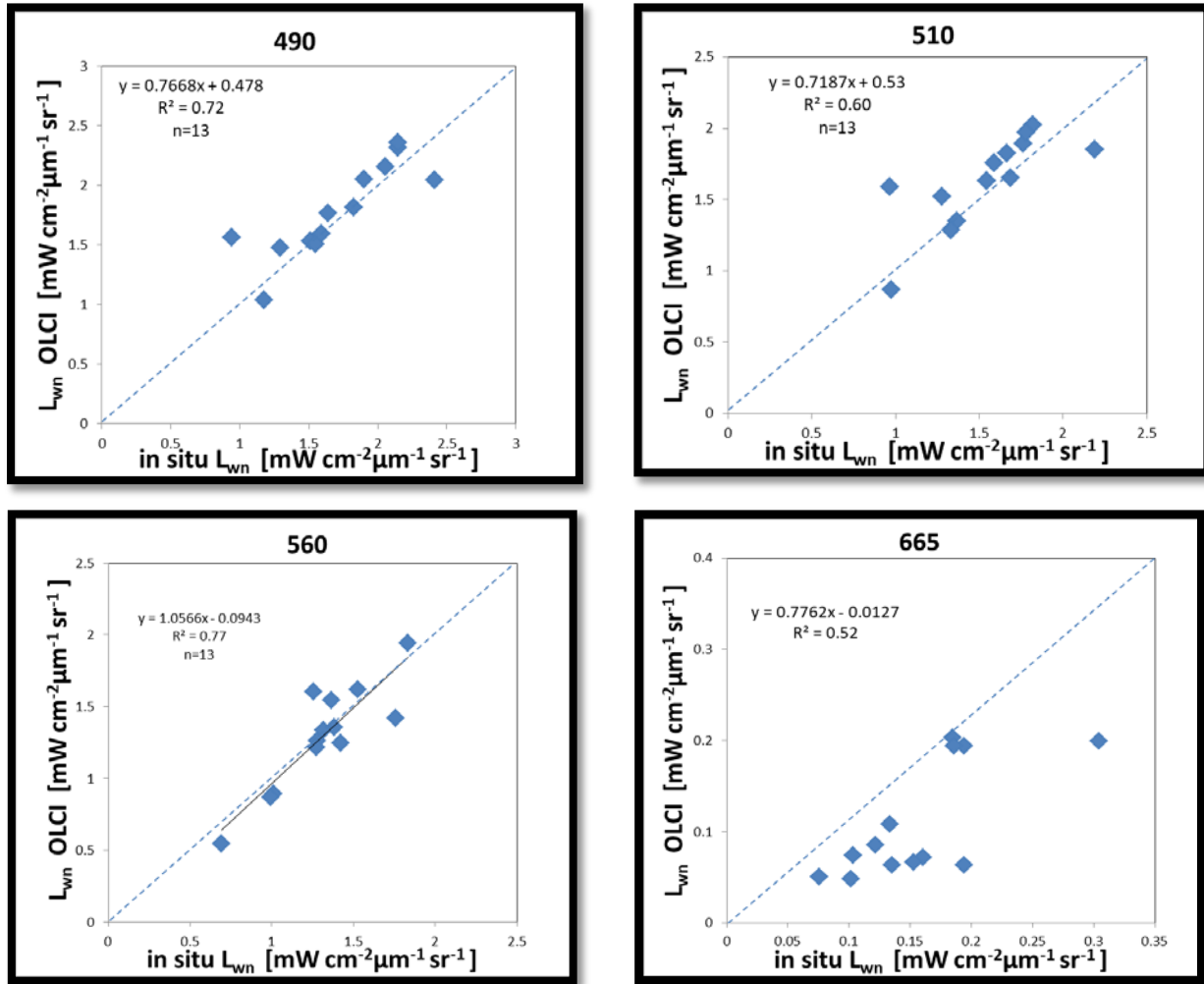


Figure 4. Scatter plots of OLCI and *in situ* L_{wn} matchup data at 412, 443, 490, 510, 560, and 665 nm

The OLCI estimates show systematic errors, thus, an underestimation of $L_{wn}(\lambda)$ showed up at 412, 443, 490, 560 and 665 nm compared to sea-truth data (Tab. 4). The positive MPD is found only for 510 nm. The highest underestimate of about -32% is estimated at 665 nm while the lowest (below 5%) occur at 443, 490 and 560 nm. Relatively low correlation of OLCI L_{wn} and *in situ* records is observed in the blue spectral band - 413 nm (Fig. 4).

Table 3. OLCIL $L_{wn}(\lambda)$ statistics

λ	MPD	MAPD	RMSE	R^2
412	-14.19	21.51	0.24	0.36
443	-3.35	13.78	0.22	0.60
490	-2.91	11.53	0.16	0.72
510	8.2	13.27	0.24	0.60
560	-2.34	12.18	0.17	0.77
665	-31.85	34.10	0.07	0.52

3.2 Assessment of the OLCI/Sentinel 3A geophysical products

✓ S3 OLCI chlorophyll products evaluation

In this report the following S3A/OLCI standard chlorophyll products were evaluated:

- **CHL_OC4ME** - chlorophyll concentration is defined by the "OC4Me" Maximum Band Ratio (MBR) semi-analytical algorithm, developed by Morel et al. [2007] following the approach of O'Reilly et al. [1998];
- **CHL_NN** - the products are derived from a NN inverse radiative transfer model, originally developed for MERIS by Doerffer and Schiller [2007], and updated to the Case 2 Regional / Coast Colour (C2RCC) processor.

The comparison between satellite derived pigments concentration and *in situ* data are based on 26 matchups (Tab. 4). The average chlorophyll concentration measured *in situ* is above 0.8 mg m⁻³. The results related to the assessment of OLCI chlorophyll products in respect to the *in situ* data are summarized in Table 5, while the scatter plots are presented on Figure 5.

Table 4. Matchup timetable

Station	Date	Time [UTM]		L _{wn} (λ)	CHL	a _{ys} (443)+ a _{npp} (443)	TSM
		in situ	overpass				
K09S52	11.06.2016	05:08	08:07	x	x	x	x
K09S53	11.06.2016	06:19	08:07	x	x	x	x
K09S54	11.06.2016	08:10	08:07	x	x	x	x
K10S66	22.06.2016	05:20	08:22	x			
K10S67	22.06.2016	06:23	08:22	x			
K10S68	22.06.2016	08:11	08:22	x			
K10S69	22.06.2016	10:13	08:22	x			
MS104	19.07.2016	05:35	08:22		x		
MSRev1	19.07.2016	07:26	08:22		x		
407	13.10.2017	05:31	08:29		x		
506	13.10.2017	10:10	08:29		x		
603	14.10.2017	10:17	08:04		x		
K2	17.10.2017	07:35	08:27		x		x
K1	17.10.2017	05:14	8:27		x		x
308	26.11.2017	08:43	07:49		x		
K11050	23.05.2019	05:37	08:11	x	x	x	
K11051	23.05.2019	07:40	08:11	x	x	x	
K11052	23.05.2019	10:07	08:11	x	x	x	
K12019	31.05.2019	06:52	08:03	x	x		

K12020	31.05.2019	08:48	08:03	x	x		
K12021	31.05.2019	10:40	08:03	x	x		
K2	12.08.2019	4:39	08:11		x		x
K1	12.08.2019	7:03	08:11		x		x
601	17.08.2019	5:08	07:57		x		
MS104	9.11.2019	5:36	08:38		x		
MS105	9.11.2019	7:25	08:38		x		
MS130	11.11.2019	5:36	08:12		x		
MS119	11.11.2019	7:03	08:12		x		
MS009	11.11.2019	8:41	08:12		x		
MS120	11.11.2019	10:47	08:12		x		

The CHL_OC4ME products show an overestimate of *in situ* chlorophyll by about 160% (MAPD), while CHL_NN is about two times lower (81.29%). A moderately good correlation ($R^2=0.65$) is observed between satellite and *in situ* data for CHL_OC4ME, whereas the CHL_NN products exhibit a determination coefficient of 0.09. The estimated log_RMSE values for both satellite products are 0.42 and 0.43 mgm^{-3} for CHL_OC4ME and CHL_NN, respectively.

Table 5. OLCI derived pigments concentration data statistics

Product	MPD	MAPD	log_RMSE	R^2
CHL_OC4ME	160.47	160.47	0.42	0.65
CHL_NN	2.77	81.29	0.43	0.09

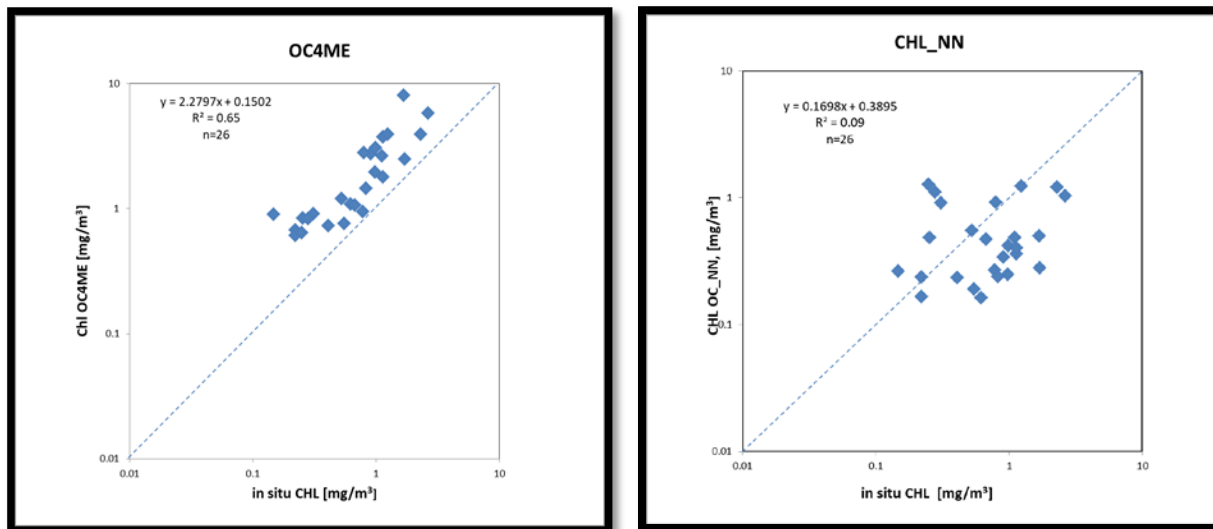


Figure 5. Scatter of OLCI derived pigments concentration [i.e., (Left) OC4ME and (Right) CHL_NN] versus *in situ* Chl a data

✓ **S3 OLCI L2 ADG 443 product evaluation**

The comparison between satellite Coloured Detrital and Dissolved Material absorption coefficient at 443 nm (ADG 443) product and *in situ* data are based on 6 matchups (Tab. 4). The *in situ* $a_{ys}(443) + a_{npp}(443)$ data used in the analysis ranged between 0.0737 to 0.1937 m^{-1} . The results related to the assessment of OLCI ADG (443) in respect to the *in situ* measurements are summarized in Table 6, and the scatter plot is presented on Figure 6.

Table 6. OLCI ADG443 data statistics

Product	MPD	MAPD	log_RMSE	R ²
ADG 443	-17.07	19.56	0.12	0.66

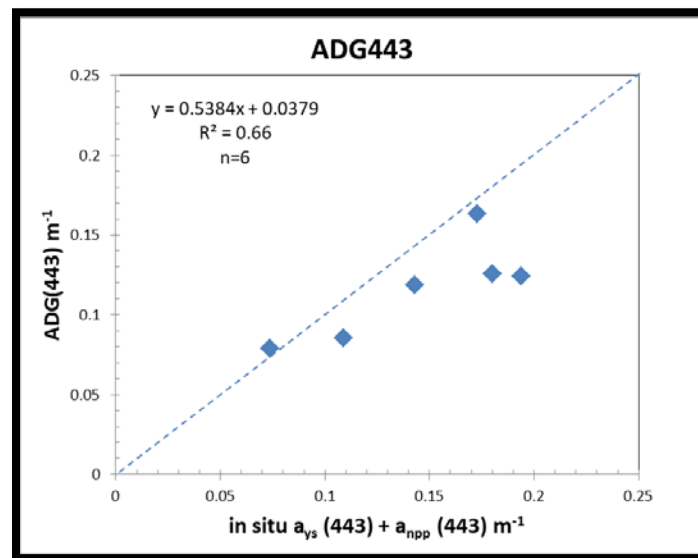


Figure 6. Scatter of OLCI ADG (443) product versus *in situ* $a_{ys}(443) + a_{npp}(443)$ data

The satellite Coloured Detrital and Dissolved Material absorption coefficient at 443 nm (ADG 443 nm) product shows an underestimate of *in situ* data by 17.07 %. The estimated log_RMSE is 0.12 m^{-1} and R² is 0.66.

✓ **S3 OLCI L2 TSM product evaluation**

The analysis of OLCI Total Suspended Matter (TSM) product and *in situ* data are based on 7 matchups (Tab. 4). The average TSM concentration measured *in situ* is 0.86 gm^{-3} . The results related to the assessment of OLCI TSM in respect to the *in situ* measurements are summarized in Table 7, and the scatter plot is presented on Figure 7.

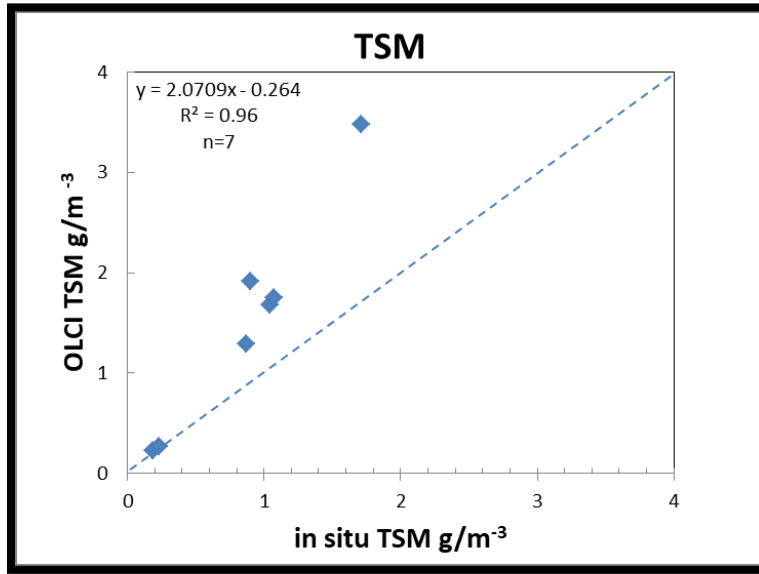


Figure 7. Scatter of OLCI ADG (443) product versus *in situ* $a_y(443) + a_{npp}(443)$ data

Table 7. OLCI TSM data statistics

Product	MPD	MAPD	log_RMSE	R ²
TSM	60.47	60.47	0.22	0.96

The S3/OLCI TSM product show an overestimate of *in situ* Total Suspended Matter concentrations by about 60% (MPD). There is a good agreement ($R^2=0.96$) between satellite and sea-truth data. The estimated log_RMSE value is 0.22 g/m⁻³.

4. Conclusions

The comparisons between satellite S3 OLCI-A Level 2 FR ocean color products and *in situ* data indicate:

- systematic underestimation of satellite normalized water-leaving radiances $L_{wn}(\lambda)$;
- overestimation of OLCI derived pigments concentration, more significant for CHL_OC4ME;
- underestimation of satellite Coloured Detrital and Dissolved Material absorption coefficient at 443 nm;
- significant overestimation of OLCI TSM product.

ACKNOWLEDGMENT

We would like to express my sincere thanks to Dr. Giuseppe Zibordi for providing the quality controlled data from Galata AERONET-OC site and for his assistance with the processing of AOP data used in this report and Dr. Jean–Francois Berthon providing us IOP data.

References

Deliverable #TN3: Bio-optical cruise report, 2019.

Doerffer, R. and Schiller, H. (2007) The MERIS Case 2 Water Algorithm. *International Journal of Remote Sensing*, 28, 517-535, doi: 10.1080/01431160600821127

EUMETSAT, “Sentinel-3 OLCI Marine User Handbook,” EUM/OPSSSEN3/MAN/17/907205, 2018a.

EUMETSAT, “Sentinel-3A Product Notice – OLCI Level-2 Ocean Colour Operational Products and Full-Mission Reprocessed Time Series,” Product notice EUM/OPSSSEN3/DOC/17/964713, 2018b.

Hooker, S.B. and C. R. McClain (2000) A comprehensive plan for the calibration and validation of SeaWiFS data. *Progress in Oceanography*, Progress In Oceanography 45(3-4): 427-465.

Morel, A. et al. (2007) Examining the consistency of products derived from various ocean color sensors in open ocean (Case 1) waters in the perspective of a multi-sensor approach. *Remote Sensing of Environment*, doi:10.1016/j.rse.2007.03.012.

O'Reilly, J. E., Maritorena, S., Mitchell, B. G., Siegel, D. A., Carder, K. L., Garver, S. A., et al. (1998) Ocean color algorithms for SeaWiFS. *Journal of Geophysical Research*, 103, 24937–2495.

G. Thuillier, M. Hersé, D. Labs, T. Foujols, W. Peetermans, Gillotay, P.C. Simon, and H.Mandel, “The solar spectral irradiance from 200 to 2400 nm as measured by the SOLSPEC spectrometer from the Atlas and Eureka missions,” *Solar Physics* 214, 1–22, 2003.

Zibordi, G., Holben, B., Slutsker, I., Giles, D., D’Alimonte, D., Mélin, F., Berthon, J.-F., Vande-mark, D., Feng, H., Schuster, G., Fabbri, B. E., Kaitala, S., and Seppälä, J. (2009a) AERONET-OC: a network for the validation of Ocean Color primary radiometric products, *J. Atmos. Ocean. Tech.*, 26, 1634–1651.

G. Zibordi, F. Mélin, J.-F. Berthon, “A regional assessment of OLCI data products,” *IEEE Geoscience and Remote Sensing Letters*, 15, 1490–1494, 2018.